

MODELING AND SIMULATION OF AN AUTOMATED MANUAL TRANSMISSION SYSTEM

Hua Huang, Sebastian Nowoisky, René Knoblich, Clemens Gühmann

Technische Universität Berlin
Department of Energy and Automation Technology
Chair of Electronic Measurement and Diagnostic Technology
Berlin 10587, Germany

{[hua.huang@campus.](mailto:hua.huang@campus.tu-berlin.de), [sebastian.nowoisky@.](mailto:sebastian.nowoisky@tu-berlin.de), [r.knoblich@.](mailto:r.knoblich@tu-berlin.de), [clemens.guehmann@.](mailto:clemens.guehmann@tu-berlin.de)}tu-berlin.de

ABSTRACT

With the continuous growth in the emission requirements and higher riding comfort demand, the shift quality takes more and more an important role in automated transmission control algorithms. In order to effectively optimize the corresponding control parameters and functions in the transmission control units (TCU), the model-based calibration is a suitable method. For this purpose a detailed dynamic model which can provide a virtual platform for shift quality optimization is imperative and necessary. In this paper a 5-speed automated manual transmission (AMT) is used as a research object and a detailed Modelica[®] based hydro-mechanical dynamic model is presented. Finally, model simulations are compared with the measurements from a test bench. Testing results show the dynamic model can describe detailed gear shifting phenomena.

Keywords: automated transmission, hydraulic, dynamic modeling

1. INTRODUCTION

With the continuous growth in the stricter emission requirements and higher riding comfort demand, the shift quality takes more and more an important role in automated transmission control algorithms. With the traditional software development process, these requirements rapidly increase the manpower and finance resources, especially the optimization period during real vehicle calibration. In order to effectively optimize the corresponding control parameters and functions in the transmission control units (TCU), the model-based calibration is a suitable method. The general process is shown in figure 1. Firstly, a formula expression based transmission model is built. By means of measurements from a test bench or a real vehicle, the draft model is detailed and improved till it reaches corresponding requirements. Afterwards, this model is taken as a virtual platform to optimize the shift quality. Finally, the optimized control parameters are verified on the test bench or in the real vehicle, the operation maps are generated and stored into the TCU.

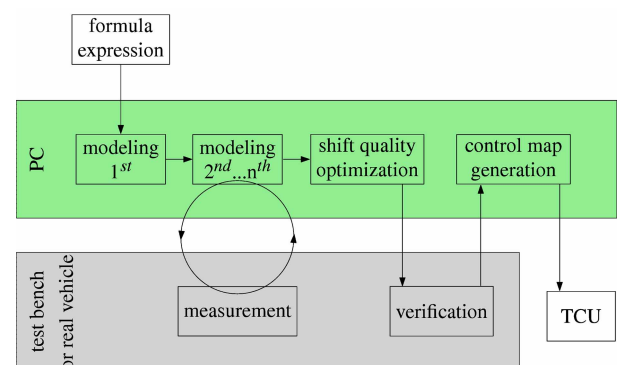


Figure 1: Model-based Optimization Process

Traditionally the shift quality is assessed subjectively by the driver's feeling. For the model-based development the shift quality objective evaluation is a critical step. This requires that the automated transmission model has a detailed performance such as speed oscillation and the longitudinal acceleration variations during a gear shifting. Only the detailed dynamic transmission model can reproduce these behaviors. Moreover, an AMT is designed and improved on the basis of a manual transmission (MT), it inherits the MT features such as lower weight, high efficiency and convenient maintenance. With the help of improved electronic technology and optimized control algorithms, AMT also offers its own advantages, such as improved driving convenience, reduction of life-cycle costs and enabled low fuel consumption.

In this paper a 5-speed AMT with dry clutch is chosen as the research object (see Figure 2). A Modelica[®] based nonlinear dynamic hydro-mechanical AMT model for the future model-based shift quality development is presented. The model is relatively simple, yet it visually describes AMT system detailed structures as “what you see is what you get” and predicts the important dynamic gear shifting behaviors quite well, such as 5 stages synchronization (pre-sync, locking, unlocking, turning hub and engagement), magnetic valve fluid pressure fluctuation under different currents and the driveline oscillation during transmitted torque changes.

The hydraulic fluid follows through the supply port, generates a force and moves the plunger to the left till the spring force is equal to the supply pressure. This stable state is called middle position. The steady-state equation is expressed in equation 1, where A_s , A_r are the effective areas of supply port and release port chambers, P_s , P_r are the supply port and release port hydraulic pressures, $F_{spring0}$ denotes the initial spring preload force.

$$F_{spring0} = P_s A_s - P_r A_r \quad (1)$$

When this magnetic valve is actuated by a current i , the coil induces an electromagnetic force $F_{magnetic}$ (see equation 2), which gives the plunger an impulse to move to the left side. During the plunger movement process, the orifice area of the supply port to output port increases and output pressure grows. Since the output port is connected with the sensing chamber, a pressured fluid is accumulated and reacts against the plunger. Besides the reaction of pressure force, the plunger is also affected by the spring force and friction. These forces take the plunger a back and forth spring-damping movement till it stops at the middle position again. Equation 2 describes the transient response,

$$\begin{aligned} \dot{x}_{plunger} &= v_{plunger} \\ m_{plunger} \dot{v}_{plunger} &= F_{magnetic} + P_s A_s - P_0 A_0 \\ &\quad - P_r A_r - P_0 A_{slider} - F_{spring} \\ &\quad - F_{spring0} - F_{friction} \\ F_{friction} &= \text{sign}(v_{plunger})(F_{coulomb} \\ &\quad + F_{prop} + F_{stribeck}) \\ F_{magnetic} &= \frac{1}{2} i^2 \frac{dL}{dx_{plunger}} + ci \end{aligned} \quad (2)$$

where $x_{plunger}$, $v_{plunger}$ and $m_{plunger}$ is plunger position, speed and mass, A_{slider} is the effective area of sensing chamber, $F_{magnetic}$ is the magnetic force induced by current i , coil inductance L and converter constant c (depends on the structure parameters such as flux density and wire length) (Modelon 2009), $F_{friction}$ is the resistance friction including constant coulomb friction $F_{coulomb}$, speed proportional friction force F_{prop} and stribeck friction $F_{stribeck}$, F_{spring} is spring force by stiffness k . If a dither signal is added into the magnetic valve control, $F_{stribeck}$ can be taken as zero.

The final steady-state is given by equation 3. In this state the plunger stops at the middle position, its velocity and acceleration are zero. The spring returns to the initial position and takes a force as large as the preload force $F_{spring0}$.

$$\begin{aligned} 0 &= F_{magnetic} + P_s A_s - P_0 A_0 \\ &\quad - P_r A_r - P_0 A_{slider} - F_{spring0} \end{aligned} \quad (3)$$

With equation 1 and equation 3 the relationship between magnetic force and sensing chamber reaction force can be expressed in equation 4. For a detailed magnetic valve the physical geometrical parameters are fixed, so the conclusion that pressure control valve command current has a linear relationship with output pressure can be accepted. This relation is described in equation 5, where m is the slope, n is the offset and i_0 denotes the initial current which is used to overcome the friction from static condition (Nowoisky 2012a).

$$F_{magnetic} = P_0 A_{slider} + P_0 A_0 = P_0 (A_{slider} + A_0) \quad (4)$$

$$P_0 = \begin{cases} 0 & i < i_0 \\ m(i - i_0) + n & i \geq i_0 \end{cases} \quad (5)$$

Fluid flow q during this process can be expressed by Bernoulli's equation (see equation 6), γ is the discharge coefficient and ρ is the density of fluid. When the plunger moves from the middle to the left position, the output port is connected to the supply port, fluid flow and its pressure level increase. When the plunger moves to the right side from the middle position, the output port is connected to the release port. This causes fluid flows to the tank. When the plunger is in the middle position, there is no flow rate except leakage, the output port pressure keeps a stable value (Merritt 1967).

$$q = \begin{cases} \gamma \sqrt{\frac{2(P_s - P_0)}{\rho}} A_s(x_{plunger}) & \text{left} \\ 0 & \text{middle} \\ -\gamma \sqrt{\frac{2(P_0 - P_r)}{\rho}} A_s(x_{plunger}) & \text{right} \end{cases} \quad (6)$$

Based on the above description, a Modelica[®] based module can be built as figure 5 shows. Its components are modeled based on the Modelica Standard Library (MSL) and hydraulic library HyLib[®] (Modelcia Association 2008, Modelon 2009). The geometrical parameters are identified through measurements, the others are fixed through experiments and calculation from theoretical and physical laws.

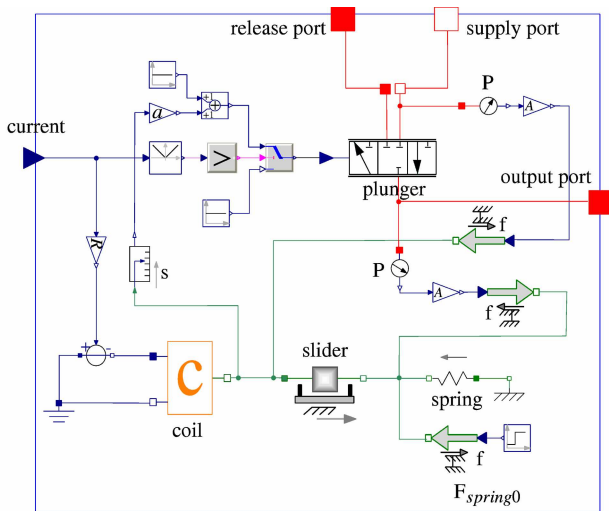


Figure 5: Dynamic Module of Pressure Control Valve

2.1.2. Mechanical Components

Synchronizers are important components in the transmission. It uses friction and locking elements to synchronize the occurring speed difference during gear shifting. As shown in figure 6, the gear shifting process can be divided into 5 stages according to the gearshift position and the difference speeds (Kiencke 2005). This division is defined under the assumption that the gearshift sleeve is at the beginning in the neutral position:

Stage 1: Gearshift force F_S causes an axial movement of the gearshift sleeve and triggers the gear shifting process. The movement stops when the synchronizer ring blocks the gearshift sleeve.

Stage 2: The axial force is transmitted from the gearshift sleeve to the synchronizer ring, resulting in a friction torque T_R , which is much larger than the gearing torque T_Z . At this stage the speed difference ΔS between the idler gear and transmission shaft is reduced to zero.

Stage 3: When the speed difference ΔS is close to zero, the friction torque T_R vanishes. At this moment the synchronizer ring turns back to release the gearshift sleeve.

Stage 4: The gearshift sleeve begins to move until it encounters the synchronizer hub external gearing. The speed difference ΔS increases again as the synchronizing torque diminishes.

Stage 5: The whole synchronization process is completed as soon as the gearshift sleeve tothing engages the synchronizer hub gearing. The power flow

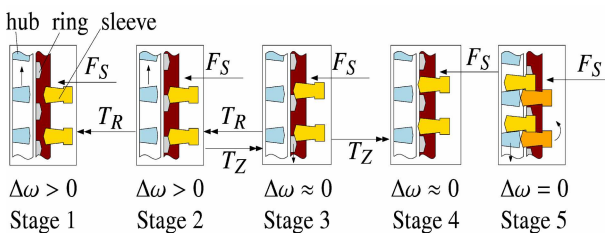


Figure 6: Synchronizing Process

is transmitted from the transmission shaft to the gear.

The torque detailed values are changed according to the synchronization stages: The friction torque T_R given by equation 7 (applied to stages 1 and 2) is calculated through the gearshift force F_S , the number of friction surfaces j and some other geometric values. The gearing torque T_Z expressed as equation 8 (used in stages 2 and 3) is calculated by gearshift force F_S , clutch diameter d_{KS} , teeth angle and friction μ_{lt} between gearshift sleeve and synchronization ring (INA 2007, Kirchner 2007). The Modelica® based synchronizer module is shown in figure 7. It is modeled based on MSL library and some new created Modelica® based blocks (such as *SynStatusCheck* block and *RingandHub* block). Detailed description and modeling process are in Huang (Huang 2012).

$$T_R = jF_S \frac{d_{ms}}{2} \frac{\sim_{ft}}{\sin \gamma} \quad (7)$$

$$T_Z = \frac{F_S d_{ks}}{2} \left(\frac{\cos \frac{S}{2} - \sim_{lt} \sin \frac{S}{2}}{\sin \frac{S}{2} + \sim_{lt} \cos \frac{S}{2}} \right) \quad (8)$$

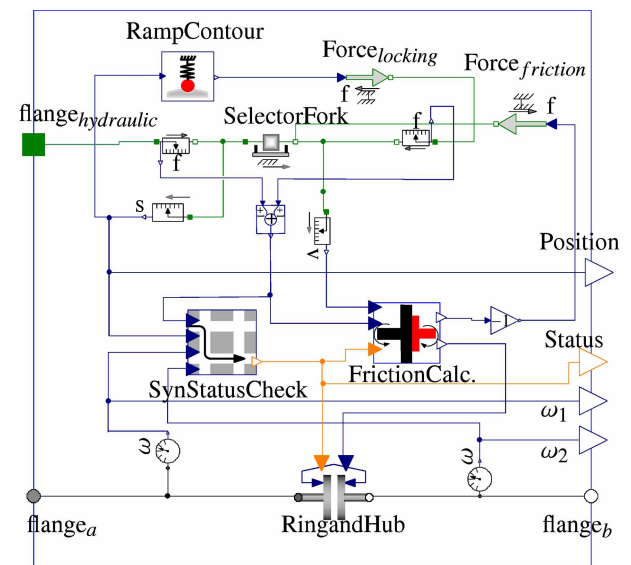


Figure 7: Dynamic Module of Synchronizer

In order to improve the dynamic behavior during gear shifting, the simplified dynamic shaft with viscous and elastic effect is necessary. The transmission shafts (crankshaft, main shaft and secondary shaft) are considered as spring-damper elements connected with inertias. The whole driveline schematic diagram is expressed in figure 8. The necessary friction losses are also added. They are modeled with lookup-tables based on experiment data.

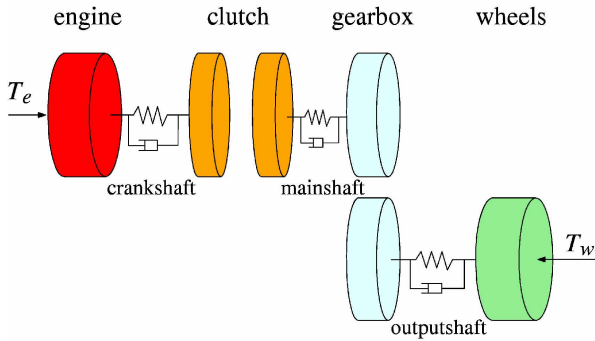


Figure 8: Schematic Diagram of Driveline

2.2. Clutch Model

Figure 9 depicts the push-type single-plate dry clutch used in the researched AMT system.

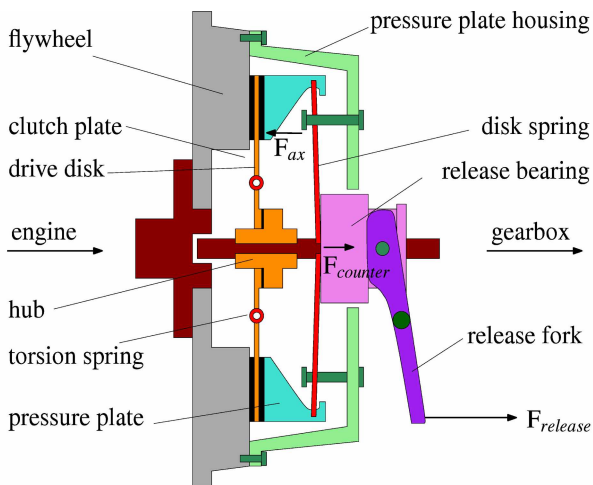


Figure 9: Schematic Diagram of Clutch

The release fork and the disk spring are used to gain an axial pressure to the release bearing and the pressure plate. The release force $F_{release}$ causes an increased normal force on the clutch plate (consists of drive disk, torsion spring, hub and etc.), the engine and the gearbox are then separated. When the force $F_{release}$ releases, the pressure plate comes close to the clutch plate, and the engine torque can be transmitted from flywheel to the gearbox through drive disk and torsion spring. Disk spring and the torsion spring are two important elements in clutch components for the gearshift quality research.

2.2.1. Hydraulic Components

A proportional valve (PVI in figure 3) is used to control the clutch cylinder movement. This dynamic process is described in equation 9. The movement depends on the mass of the cylinder piston m_{piston} , acceleration a_{piston} , piston area A_{piston} , pressure P , the friction force $F_{friction}$ (mentioned in equation 2) and the counterforce $F(s)$ from the mechanical clutch component.

$$m_{piston} a_{piston} = PA_{piston} - F_{friction} - F(s) \quad (9)$$

The derivation of piston pressure is calculated through equation 10, where K is compressibility modulus and V_0 is the offset volume due to hydraulic feed line.

$$\dot{P} = \frac{K}{V_0 + A_{piston} x_{piston}} (q - A_{piston} v_{piston}) \quad (10)$$

The proportional valve has the feature that the opening area A_{pv} has a linear response to the input current i . The causing volume flow q expression is similar to equation 6 (the valve opening area is controlled by the electric current i rather than plunger position $x_{plunger}$).

2.2.2. Mechanical Components

The clutch capacity describes the characteristic of the torque transmitted over the clutch while the sliding stage. It is expressed in equation 11,

$$T_c \approx F_{ax} \sim z \frac{2(r_0^3 - r_i^3)}{3(r_0^2 - r_i^2)} \quad (11)$$

with axial force F_{ax} on the friction lining, speed depended friction coefficient μ , friction surfaces plates number z , outer and inner friction surface radius r_0 and r_i . It is worth noting that during the clutch slipping phase, the clutch transmitted torque equals to the clutch capacity. When the clutch engages (becomes a coupling system), the torque equals to the engine torque minus engine friction losses. For simplification, the release bearing axial displacement is used as module input for the calculation of clutch capacity, and the relationship between clutch transmitted torque and release bearing axial displacement is depicted by a lookup-table generated through experiment (Nowoisky 2013). The release bearing axial counterforce $F_{counter}$ is a resultant force of disk and coat springs. It can be obtained from axial force F_{ax} under the assumption that the disk spring is a stiff lever. But actually the disk spring has a variable stiffness depends on the compressed clutch position. A lookup-table, which avoids the stiff lever transformation problem, is used to describe this counterforce when releasing bearing has an axial displacement.

The clutch torsion damping system is used to reduce rotational irregularities induced by internal combustion engines (Luk 2012). This element is significant for the dynamic model in the purpose of shift comfort calibration. The clutch torsion damping system is modeled with a spring-damping system (multiple compression springs and a damper). Figure 10 depicts the torsion spring characteristic. When the relative angle Δ_n begins from zero, the smaller spring with stiffness k_l is firstly compressed (this process is used for vehicle idle operations), after the relative angle reaches Δ_{n1} , the smaller spring is fully compressed, and the stiffer

spring with stiffness k_2 starts to be compressed (this process is used for vehicle driving operations). When Δ_{r_2} reaches, springs are stopped to be compressed and comes to a mechanical stop (Naunheimer 2011, Drexl 1997). The Modelica[®] based clutch module is shown in figure 11. Its mechanical components are modeled with MSL library and hydraulic components are modeled with HyLib[®] library. The corresponding parameters are fixed through measurements and test bench experiments.

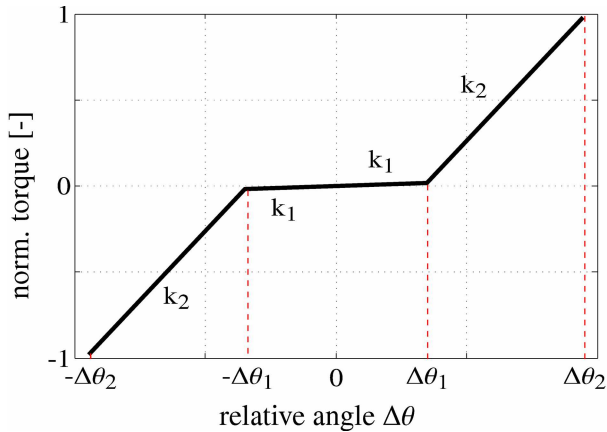


Figure 10: Torsion Spring Characteristic

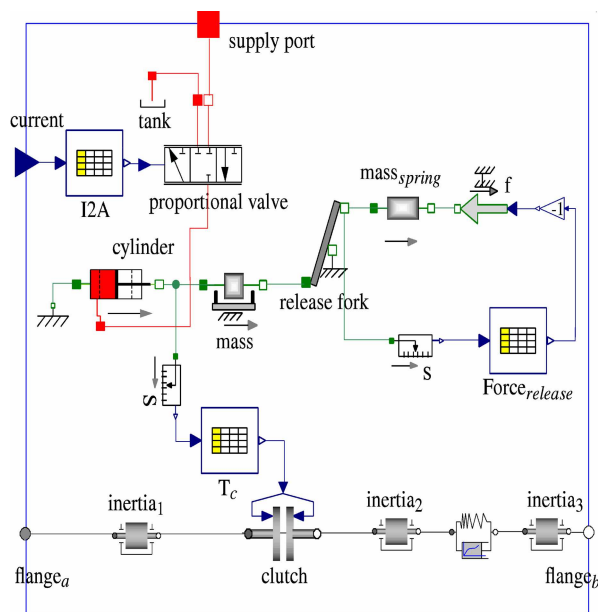


Figure 11: Dynamic Module of Clutch System

3. MODEL SIMULATION

In order to verify the rationality and effectiveness of this dynamic model, some tests are carried out. These simulations are carried out with Dymola[®] DASSL (differential-algebraic system solver) integration Algorithm, tolerance setting is 0.0001 (Dynasim AB 2010). Detailed testing results of synchronizers can be found in Huang (Huang 2012).

Figure 12 shows the pressure control valve output pressure responses under different step currents beginning at 0.05 s. The output pressure firstly has an overshoot which is generated by current, and then the

plunger takes a back and forth spring-damping movement till it stops at middle position (see figure 4), so the output pressure takes an oscillation at the beginning and then keeps a stable value at the end. When the input command current value is less than 600 mA, the valve output pressure is zero since the impulse cannot overcome the fluid viscosity and some other friction.

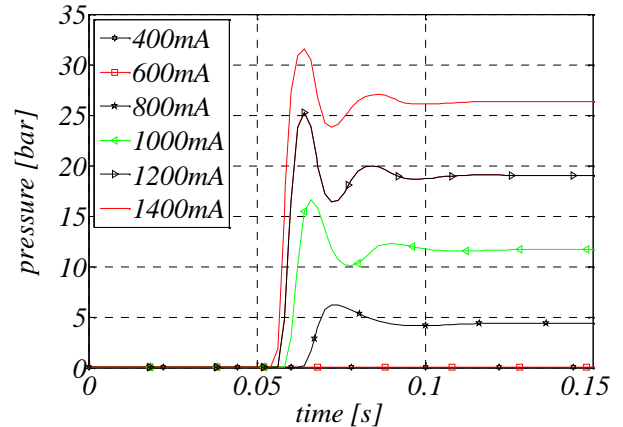


Figure 12: Simulation Result of Pressure Control Valve

Finally, the model is compared with measurement data from an AMT equipped test bench (Knoblich 2011, Nowoisky 2012b). Two three-phase asynchronous motors are used as drive and load engine. In this testing the drive engine and load engine were set in constant torque mode, 10 Nm and -20 Nm. After the system has reached the steady-state, the clutch was totally opened and gear was shifted from neutral position to 1st gear, then the clutch was closed in a ramp mode. For the simulation model the magnetic valves were triggered with the same signals as those of the test bench. The shafts of the model input and output are connected with the constant torque values of 10 Nm and -20 Nm. The comparison results are shown in figure 13. If the drive motor has a positive torque, the engine speed and gearbox input speed at the beginning have a positive value (figure 13 (a) and (b)). For the same reason the gearbox output rotates with a negative value (figure 13 (c)). At 1 s the clutch begins to open (figure 13 (e)) and subsequently the gear shifts (figure 13 (d)), the gearbox input speed decreases and synchronizes with the output speed. Afterwards, at 2 s the clutch closes in a ramp mode (figure 13 (e)), engine speed and gearbox input speed begin to engage (at 4 s). Since the torque transferred from the drive engine is larger than the one from the load torque, the input speed increases to a positive value again (figure 13 (b)). From the comparison it can be seen the model can accurately reproduce the gear shifting process and the normalized root mean square errors (NRMSE, see equation 12) are below 10%. Moreover, this model describes the important shifting behavior for the shift quality evaluation (e.g. the speed oscillation during the clutch engagement) and expresses the influences with different control variants (e.g. the change trend of the clutch

cylinder pressure), these shifting phenomena are not possible to be represented through a very simple model. The CPU-time costs 0.88 seconds for this simulation (7 seconds) under a quad-core processor.

$$e_{NRMS} = \sqrt{\frac{1}{N} \sum_{i=1}^N \left(\frac{y_{meas} - y_{sim}}{\max(y_{meas}) - \min(y_{meas})} \right)^2} \quad (12)$$

4. SUMMARY AND OUTLOOK

This paper gives a detailed introduction to AMT system working principles, presents a relative simple but effective Modelica[®] based dynamic model. The shift behaviors are also successfully verified through experimental data. This model has following features:

1. Represents a detailed AMT gear shift process, describes synchronization process with 5 stages.
2. Describes detailed hydro-mechanical actuators, represents the pressure control valve dynamic response.
3. Models torsion damping system in clutch and spring-damping system in driveline, which makes speed oscillation during torque changes possible. This improves dynamic model closer to a real one.
4. Detailed expresses the relationships between the control parameters and the shift process, this makes the model-based calibration possible.
5. Develops a multi-domain model, dynamically integrates hydraulic and mechanical systems together.
6. The model is developed based on Modelica[®], it

describes the system in a physical perspective. This makes other co-developer or user more easily to understand the physical meaning.

7. The tested AMT modules have a good modularity for other similar systems setups only through parameters changes.
8. Supplies a complete virtual AMT system platform for future mode-based shift quality calibration.

Based on the above description and comparison, this dynamic nonlinear model makes model-based shift quality calibration on automated transmissions possible.

REFERENCES

- Volkswagen AG, 1999. *Self-study Programme 221: Electronic Manual Gearbox, Design and Function*. Volkswagen AG.
- Modelon, 2009. *HyLib (2009), version 2.7*. Product help, Modelon, 2009.
- Nowoisky, S., Knoblich, R., and Gühmann, C., 2012a. Comparison of Different Model Types based on a Synchronization of an Automated Manual Transmission. *Proceedings of Simulation und Test für die Automobilelektronik IV*, 38-47. 2012, Berlin.
- Merritt, H. E., 1967. *Hydraulic Control Systems*. USA: John Wiley & Sons, Inc.
- Modelica Association, 2008. *Modelica Standard Library (2008), version 3.1*. Product help, Modelica Association.
- Kiencke, U., Nielsen, L., 2005. *Automotive Control Systems: For Engine, Driveline, and Vehicle, 2nd edition*. Germany: Springer.
- INA, 2007. *Intermediate Rings for Multi-Cone Synchronizer Systems*. Schaeffler Technologies

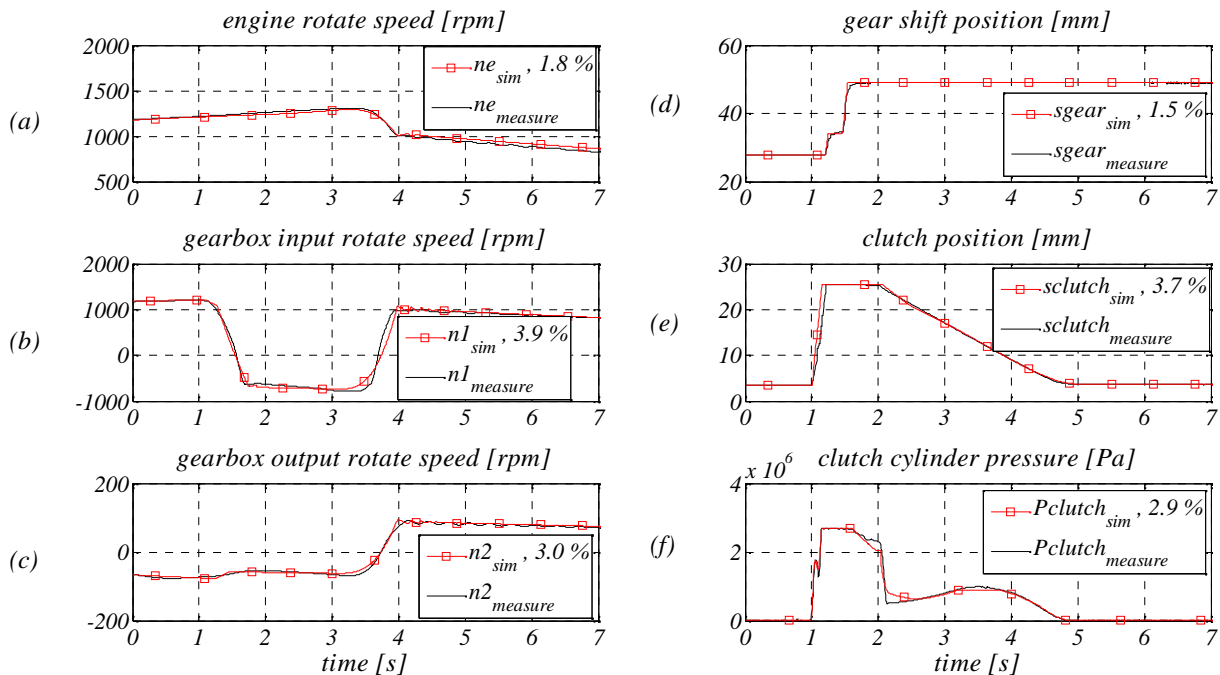


Figure 13: Comparison of Shifting Process with Measurements

AG & Co. KG.

- Kirchner, E., 2007. *Leistungsübertragung in Fahrzeuggetrieben: Grundlagen der Auslegung, Entwicklung und Validierung von Fahrzeuggetrieben und deren Komponenten* (in German). Germany: Springer.
- Huang, H., Nowoisky, S., Knoblich, R., and Gühmann, C., 2012. Modeling and Testing of the Hydro-mechanical Synchronization System for a Double Clutch Transmission. *Proceedings of the 9th International Modelica Conference*, 284-294. 2012, Germany.
- Nowoisky, S., Gühmann, C., 2013. Automated Parameter Identification for a Dry Clutch. *Proceeding of 10th International Multi-Conference on Systems, Signals & Devices (SSD)*, 18-21. 2013, Tunisia.
- Luk, 2012. *Luk Clutch Course: An Introduction to Clutch Technology for Passenger Cars*. Schaeffler Automotive Aftermarket GmbH & Co. KG.
- Naunheimer, H., Bertsche, B., Ryborz, J., Novak, W., 2011. *Automotive Transmissions: Fundamentals, Selection, Design and Application, 2nd edition*. Germany: Springer.
- Drexl, H.-J., 1997. *Kraftfahrzeugkupplungen: Funktion und Auslegung* (in German). Germany: Moderne Industrie.
- Dynasim AB, 2010. *Dymola (2010), version 7.4*. Product help, Dynasim AB.
- Knoblich, R., Beilharz, J., and Gühmann, C., 2011. Modellbasierte Steuergeräteentwicklung für Kfz-Getriebesysteme am Prüfstand (in German). *In Tagungsband Mechatronik*, 191-196. 2011, Dresden.
- Nowoisky, S., Knoblich, R., and Gühmann, C., 2012b. Prüfstand für die Identifikation und den Funktionstest an automatisierten Schaltgetrieben (in German). *In Virtuelle Instrumente in der Praxis*, 150-156. 2012, Germany.